



New records of endophytic fungi from *Phragmites australis* in Iran

F. Salimi

M. Javan-Nikkhah✉

Department of Plant Protection, College of Agriculture and Natural Resources, Faculty of Agriculture, University of Tehran, Karaj, Iran.

A. Alizadeh

Department of Plant Protection, Faculty of Agriculture, Azarbaijan Shahid Madani University, Tabriz, Iran.

A. Mirzadi Gohari

Department of Plant Protection, College of Agriculture and Natural Resources, Faculty of Agriculture, University of Tehran, Karaj, Iran.

M. Thines

Biodiversity and Climate Research Centre (BiK-F), Senckenberg Gesellschaft für Naturforschung, Senckenberganlage 25, D-60325 Frankfurt am Main, Germany and Goethe University, Institute of Ecology, Evolution and Diversity, Max-von-Laue-Str. 13, D-60438 Frankfurt am Main, Germany.

Abstract: In order to contribute to the knowledge of endophytic fungi of *Phragmites australis* (Poaceae) in Iran, seventeen isolates were recovered from the leaves, stems and roots of healthy common reed plants collected from five different sites around Lake Urmia in the East and West Azarbaijan provinces, Iran. Five different species viz *Achroiostrachys betulicola*, *Ac. humicola*, *Cephalotrichum tenuissimum*, *Myrmecridium schulzeri*, and *Priconia igniaria* were identified based on morphological characteristics and phylogeny inferred from nuclear internal ribosomal transcribed spacer sequence (ITS-rDNA). To the best of our knowledge, this is the first report of *Ac. betulicola* and *Ac. humicola* for the Funga of Iran. In addition, this study provided new insights into the distribution and host range of the identified species.

Key words: Ascomycota, Biodiversity, Lake Urmia, phylogeny, Poaceae, symbiosis.

INTRODUCTION

Fungal endophytes are a unique group of plant symbionts that live locally and sometimes systematically in plant internal tissues over longer timespans without triggering disease symptoms (Salimi et al. 2019; Singh et al. 2021; Yadav et al. 2021). Some enhance the fitness of their host plant, while also benefiting from this interaction in receiving nutrients and protection from the host plant (Preethi et al. 2021; Baron & Rigobelo 2022). The beneficial features and positive aspects of endophytic fungi on their host plants have been discussed in numerous studies (Busby et al. 2016; Card et al. 2016; Vega 2018; Quesada-Moraga 2020). They range from enhancing plant growth by helping to absorb minerals and increasing plant resistance to alleviating various biotic and abiotic stresses such as plant pathogens, herbivores, drought, salinity, metal toxicity, temperature extremes, and pH (Breen 1994; Brem and Leuchtmann 2001; Schulz et al. 2002; Clay & Schardl 2002; Hyde & Soytong 2008; Rodriguez et al. 2008; Cheplick et al. 2009; Kipfer et al. 2011; Atala et al. 2022; Verma et al. 2013; Soares et al. 2016; Salimi et al. 2019). Therefore, they are considered key components of natural ecosystems. Endophytic fungi have been widely reported from many plant species around the world, including habitats as diverse as arctic environments, deserts, the sublittoral, perhumid tropics, and mangrove swamps (Fisher et al. 1995; Redman et al. 2002; Strobel 2002; Bashyal et al. 2006; Suryanarayanan et al. 2005; Wang et al. 2006; Li et al. 2008; Rosa et al. 2009).

During the past two decades, much attention has been paid to these microorganisms, including their biodiversity, ecology, and biotechnology, with special emphasis on the possible use of these microorganisms in agriculture as biological control agents and biofertilizers. Hundreds of novel fungal species have been isolated as plant endophytes and described in the last decades (Liu et al. 2007; Zhang et al. 2007; Novas and Carmarón 2008; Bills et al. 2012; Meshram et al. 2013; Tao et al. 2013; Harrington et al. 2019; Silva et al. 2019; Tanney & Seifert 2019;

Submitted 22 Oct 2022, accepted for publication 9 April 2023

✉ Corresponding Author: E-mail: jnikkhah@ut.ac.ir

© 2023, Published by the Iranian Mycological Society

<https://mij.areeo.ac.ir>

Ibrahim et al. 2020; Noumeur et al. 2020; Zheng et al. 2022). It is estimated that more than 200 different bioactive compounds have been discovered from these microorganisms, and more of these potentially valuable metabolites are likely to be discovered in the future.

Common reed (*Phragmites australis* (Cav.) Trin. Ex Steud.) is a perennial plant that has successfully occupied a wide range of natural and agricultural habitats worldwide (Kowalski et al. 2015, Meyerson et al. 2018, Salimi et al. 2019). It can withstand a wide range of abiotic stresses and extreme conditions such as salinity, heavy metal toxicity, temperature range, pH range, and mineral deficiency (Achenbach & Brix 2014; Bonanno & Giudice 2010). Besides the ecological and physiological capacities of common reed (Fer & Hroudova 2009; Meyerson et al. 2016), it is estimated that an important key to its success in expanding globally is the symbiotic relationship of this plant with various endophytic microorganisms (Kowalski et al. 2015; Rodriguez et al. 2008, Sangamesh et al. 2018).

This study was conducted with the aim of expanding the knowledge of endophytic fungi of *Ph. australis* by investigating their presence in different sites around Lake Urmia in Iran.

MATERIALS AND METHODS

Sample collection

Samplings of healthy *Ph. australis* plants were carried out from the five different locations around Lake Urmia, in the East and West Azarbaijan provinces, Iran, during the summer and autumn of 2018. At each sampling location, ten intact plants (height 1.5-3.0 m) with undamaged leaves, roots and rhizomes were randomly collected, transported to the laboratory in polythene bags and processed for the isolation of endophytic fungi on the same day or within a maximum of 48 hours following standard techniques (Rodriguez et al., 2008; Salimi et al. 2019). The samples were washed in running water to remove dust and debris for 15 mins, air-dried, and then cut into approximately 1 cm pieces. For surface sterilization, plant parts were subjected to treatment with several solutions in a beaker, applying gentle shaking. First, they were soaked in 70% ethanol for 1 min, then in sodium hypochlorite (3% available chlorine) with 0.1% of Tween 20 for 2 mins for leaves and stems and 3 mins for root segments. Afterward, samples are submersed in 70% ethanol for 1 min and subsequently rinsed five times with autoclaved distilled water (a modified method of Rodriguez et al., 2008). After this, samples were plated on both Petri dishes containing potato dextrose agar (PDA, Merck, Darmstadt, Germany) and 2% water agar (WA, 2%), both supplemented with chloramphenicol (20 µg/ml) and streptomycin (50 µg/ml). Petri dishes were kept in the dark at 20-25 °C for 7-21 days. WA plates supplemented with chloramphenicol (20 µg/L) were inoculated with fungal mycelium/structures formed on WA and PDA plates. Purified single spore isolates

were achieved by the hyphal tip cutting method (Tutte 1969). Pure cultures were deposited in the mycology laboratory of the Faculty of Agriculture and Natural Resources, University of Tehran, Karaj, Iran (Table 1).

Morphological characterization

Both cultural and microscopic features were examined on potato dextrose agar (PDA) based on the method used by Salimi et al. (2019). Cultures were inoculated with 5 mm diameter plugs from 4–7-day-old cultures. PDA cultures were incubated for 14 days at 24 °C under dark condition. Measurements and photomicrographs of fungal structures were made based on Arzanlou et al. (2007) for *Achroiostachys* and *Myrmecridium* isolates. Likewise, *Cephalotrichum* and *Periconia* isolates were morphologically characterized following the studies of Woudenberg et al. (2017) and Yang et al. (2022), respectively. Microscopic preparations were made in clear lactic acid (0.1%), with at least 30 measurements per structure, and observed with a DIC light microscope (Imager2, Carl Zeiss, Göttingen, Germany) equipped with a Zeiss AxioCam MRc5 camera (Carl Zeiss, Göttingen, Germany). Fungal structures were measured on calibrated images using AxioVision software (Carl Zeiss, Göttingen, Germany). Colony characteristics were documented on PDA after 10 days. The growth rate was measured after seven and ten days.

Phylogenetic analysis

Genomic DNA was extracted using a modified CTAB-based method (Aboul-Maaty, & Oraby 2019). The quality of extracted DNA was determined by electrophoresis using 1% agarose gel. The 5.8S nuclear ribosomal RNA gene with its two flanking internal transcribed spacers (ITS) was amplified using the ITS1/ITS4 primers designed by White et al. (1990), following protocols described therein. Amplicons were sent for sequencing at the Senckenberg Biodiversity and Climate Research Centre, Frankfurt am Main (SBiK-F, Germany), using the primer pair used for PCR. Geneious (version 5.6) was used for viewing, editing, and assembling sequences.

Sequences were compared to other DNA sequences, particularly from ex-type and reference strains from previous studies (Table S1), obtained from GenBank (<http://ncbi.nlm.nih.gov/genbank>) using the BLAST tool (<https://blast.ncbi.nlm.nih.gov/Blast.cgi>). Sequences with the highest similarity were added to the alignment as reference strains (Fig. 1). Alignments were performed with the Q-INS-i algorithm (Katoh et al., 2013) in the latest available version, as implemented on the MAFFT web server (Katoh et al., 2019). After removing leading and trailing gaps, phylogenetic analyses were performed on the TrEase web server (<http://thines-lab.senckenberg.de/trease/>) using RAxML (Stamatakis 2014) for maximum likelihood, FastTree2 (Price et al. 2010) for Minimum Evolution and MrBayes (Ronquist et al. 2012).

Table 1. Endophytic fungal isolates recovered from *Phragmites australis*, were used for morphological characterization and phylogenetic analysis.

Species	Isolate	Host tissue	Locality		Date	GenBank accession no.
			Province/Region	GPS		ITS
<i>Achroistachys betulicola</i>	FS-N3P6R2	Root	East Azarbaijan /Sharafkhane	38.11361, 45.28190	Oct-2018	OQ780891
<i>Achroistachys betulicola</i>	FS-N4P10L5	Root	East Azarbaijan /Sharafkhane	38.11361, 45.28190	Oct-2018	OQ780890
<i>Achroistachys humicola</i>	FS-S3P3R9	Root	West Azarbaijan/ Miandoab	37.093850, 45.900982	Sep-2018	OQ780892
<i>Achroistachys humicola</i>	FS-S3P3R7	Root	West Azarbaijan /Miandoab	37.093850, 45.900982	Oct-2018	OQ780894
<i>Achroistachys humicola</i>	FS-S3P4R5	Root	West Azarbaijan /Miandoab	37.093850, 45.900982	Oct-2018	OQ780893
<i>Myrmecridium schulzeri</i>	FS-N1P6S1	Root	East Azarbaijan /Sharafkhane	38.11361, 45.28190	Oct-2018	OQ780896
<i>Myrmecridium schulzeri</i>	FS-UN7	Root	East Azarbaijan /Sharafkhane	38.11361, 45.28190	Oct-2018	OQ780895
<i>Cephalotrichum tenuissimum</i>	FS-W4P4R3	Root	West Azarbaijan /Urmia	37.44020, 45.12455	Oct-2018	OQ780897
<i>Periconia igniaria</i>	FS-N4P10L3	Leaf	East Azarbaijan /Sharafkhane	38.11361, 45.28190	July-2018	OQ780902
<i>Periconia igniaria</i>	FS-N3P7L4	Leaf	East Azarbaijan /Sharafkhane	38.11361, 45.28190	July-2018	OQ780904
<i>Periconia igniaria</i>	FS-N6P4L2	Leaf	East Azarbaijan /Sharafkhane	38.11361, 45.28190	July-2018	OQ780906
<i>Periconia igniaria</i>	FS-N3P4R10	Root	East Azarbaijan /Sharafkhane	38.11361, 45.28190	July-2018	OQ780905
<i>Periconia igniaria</i>	FS-N3P8S1	Stem	East Azarbaijan /Sharafkhane	38.11361, 45.28190	July-2018	OQ780898
<i>Periconia igniaria</i>	FS-N3P3S2	Stem	East Azarbaijan /Sharafkhane	38.11361, 45.28190	July-2018	OQ780900
<i>Periconia igniaria</i>	FS-N3P4R8	Root	East Azarbaijan /Sharafkhane	38.11361, 45.28190	July-2018	OQ780901
<i>Periconia igniaria</i>	FS-N3P2R1	Root	East Azarbaijan /Sharafkhane	38.11361, 45.28190	July-2018	OQ780903
<i>Periconia igniaria</i>	FS-N3P2L3	Leaf	East Azarbaijan /Sharafkhane	38.11361, 45.28190	July-2018	OQ780899

For Bayesian inference, each in the latest available version. For the Bayesian analysis, a GTR model was selected and the analyses were run on random trees for 1,000,000 generations, discarding 30% of the first trees as burn-in steps of the analysis to determine posterior probabilities from the remaining trees. RAxML and FastTree2 trees were drawn by choosing GTRGAMMA and GTR algorithms, respectively, and the reliability of the inferred tree was estimated by bootstrap analysis with 1000 replications. The sequences obtained in this study were deposited in GenBank and their accession numbers are given in Table 1.

RESULTS

Phylogeny

In the ITS alignment, 103 strains including 17 isolates obtained in this study, 86 reference sequences from GenBank as well as two outgroup taxa, and 652

characters including alignment gaps were processed, of which 387 characters were variable and 265 constant characters. The tree obtained from Bayesian analyses confirmed the tree topology obtained with Minimum Evolution. Most of the Bayesian posterior probability values were congruent with bootstrap support values (Fig. 1). The seventeen recovered isolates from *P. australis* investigated in this study were separated into five well-supported distinct clades with ex-type strains belonging to five known species namely *Achroistachys betulicola*, *Ac. humicola*, *Cephalotrichum tenuissimum*, *Myrmecridium schulzeri* and *Periconia igniaria*. Isolates FS-N3P6R2 and FS-N4P10L5 were placed in a clade with *Ac. betulicola*, and isolates FS-S3P3R9, FS-S3P3R7 and FS-S3P4R5 with *Ac. humicola* with high support values (1.100, respectively). Similarly, FS-W4P4R3 grouped with *C. tenuissimum* and FS-N1P6S1 and FS-UN7 isolates with *M. schulzeri* (1/100 and 1/98, respectively). Likewise, nine further

isolates, FS-N4P10L3, FS-N3P7L4, FS-N6P4L2, FS-N3P4R10, FS-N3P8S1, FS-N3P3S2, FS-N3P4R8, FS-N3P2R1, FS-N3P2R1 and FS-N3P2L3 grouped with *P. igniaria* (-/0.75). Many other species in the tree formed well-supported clades and were well-separated from closely related species.

Taxonomy

Based on the combination of morphology and phylogeny inferred by the rDNA-ITS sequence, seventeen endophytic isolates obtained from common reed were identified as five species (Table 1), including *Achroiostrachys betulicola*, *Ac. humicola*, *Cephalotrichum tenuissimum*, *Myrmecridium schulzeri* and *Periconia igniaria*. Comprehensive morphological descriptions and illustrations are provided for the species.

***Achroiostrachys betulicola* L. Lombard & Crous, Persoonia 36: 173 (2016). Fig. 2.**

Culture characteristics. Colonies on PDA flat, with entire margin, reaching 50 mm diam in 10 d at 25 °C, surface white to off-white, generally with immersed mycelia, conidiophores abundantly forming on the media, slimy masses of hyaline conidia forming at the top of conidiophores, reverse on PDA off-white.

Conidiophores macronematous, mononematous, single or in groups, erect, straight, unbranched, septate, thin-walled, smooth-walled, hyaline, 36–80 × 3–4.5 µm, bearing solitary or reel of 2–4 conidiogenous cells at the apex. Conidiogenous cells are hyaline, elongated, ampulliform to subcylindrical, forming terminally at the apex of conidiophores, 8.5–10 × 3–5 µm, with a slightly protruding apical opening. Conidia hyaline, aseptate, globose to ellipsoidal, smooth-walled, 8–12 × 5.5–7 µm, mean = 10 × 6 µm, containing 1–2 large guttules, rounded at both ends or with a rounded base and acute apex.

Specimens examined. IRAN. East Azarbaijan: Sharafkhane, from the root of *Phragmites australis*, Oct-2018, Fatemeh Salimi & Alireza Alizadeh, culture FS-N4P10L5; IRAN. East Azarbaijan: Sharafkhane, from the root of *Ph. australis*, Oct-2018, Fatemeh Salimi & Alireza Alizadeh, culture FS-N3P6R2.

Notes: The isolates examined in this study show similar morphology to that described by Lombard et al. (2016) for *Achroiostrachys betulicola*. In blastn searches on NCBI GenBank, the ITS sequence of FS-N3P6R2 and FS-N1P10L5 isolates matched with 100% and 99.82% identity to an ex-type strain of *Ac. betulicola* (CBS 136397).

The isolates FS-N1P10L5 and FS-N3P6R2 confidently clustered with the valid reference strains and the type strain of *Achroiostrachys betulicola* (CBS 136397) in both Bayesian and Minimum Evolution trees (Fig. 1). *Ac. aurantisporea* and *Ac. saccharicola* have the closest relationship with *Ac. betulicola* in the trees (Fig. 1), but the ITS-rDNA could well delineate this species from those and all accepted taxa in the genus *Achroiostrachys*.

Achroiostrachys betulicola can be morphologically distinguished from other species of the genus by the

formation of slightly larger conidia and also by the height of the conidiophores. Conidiophores of *Ac. betulicola* are shorter than those of *Ac. saccharicola* (up to 85 µm in *Ac. betulicola* vs. up to 140 µm in *Ac. saccharicola*), but longer than those of *Ac. phyllophila* (up to 70 µm), *Ac. levigata* (up to 75 µm) and *Ac. humicola* (up to 65 µm).

Just a few reports from *Ac. betulicola* are available worldwide, as listed in the USDA fungal database (Farr and Rossman 2021), of the fungus was reported from *Bambusa vulgaris* in Spain, *Betula lutea* in Canada, *Triticum aestivum* in the United States of America and *Zea mays* in Germany. The results of this study show that *Ac. betulicola* is not restricted to the previously reported regions, and its strains originate from different hosts belonging to divergent plant families, Poaceae and Betulaceae, and from three continents (North America, Europe, and Asia). These results indicate an even wider host range and greater distribution of this species than previously known, which may include other countries between the former distribution areas. However, this still needs to be confirmed by further investigations.

***Achroiostrachys humicola* L. Lombard & Crous, Persoonia 36: 173 (2016). Fig. 3.**

Culture characteristics. Colonies on PDA flat with entire margin, reaching 50 mm diam in 10 d at 25 °C, surface white to pale luteous to rosy buff, generally with abundant aerial mycelia, conidiophores abundantly forming on the aerial mycelium and surface of the medium, slimy masses of hyaline conidia forming at the top of conidiophores, reverse on PDA buff.

Conidiophores macronematous, mononematous, single or in bunches, erect, straight, unbranched, 1–2-septate, thin-walled, smooth-walled, hyaline, 33–62 × 3.5–5 µm, bearing solitary or reel of 2–6 conidiogenous cells at the apex. Conidiogenous cells are hyaline, elongated, ampulliform to ventricose, forming terminally at the apex of conidiophores, 8–11.5 × 3.5–5 µm, with a slightly protruding apical opening. Conidia hyaline, aseptate, globose to ellipsoidal, smooth-walled, 7–10 × 5.5–7 µm, mean = 8.5 × 6 µm, containing 1–2 large guttules, rounded at both ends or with a rounded base and acute apex.

Specimens examined. IRAN. West Azarbaijan: Miandoab (37.093850, 45.900982), from the root of *Ph. australis*, Sep-2018, Fatemeh Salimi & Alireza Alizadeh, culture FS-S3P3R9; IRAN. West Azarbaijan: Miandoab (37.093850, 45.900982), from the root of *Ph. australis*, Sep-2018, Fatemeh Salimi & Alireza Alizadeh, culture FS-S3P3R7; IRAN. West Azarbaijan: Miandoab (37.093850, 45.900982), from the root of *Ph. australis*, Sep-2018, Fatemeh Salimi & Alireza Alizadeh, culture FS-S3P4R5.

Note: The isolates examined in this study show similar morphology to that described by Lombard et al. (2016) for *Achroiostrachys humicola*. In blastn searches in NCBI GenBank, the ITS sequence of isolates FS-S3P3R7 and FS-S3P4R5 matched with

99.82% and isolate FS-S3P3R9 with 99.45% identity to an ex-type strain *Ac. humicola* (CBS 868.73).

The studied isolates were confidently clustered with reference strains and the type strain of *Ac. humicola* (CBS 868.73) in both Bayesian and Minimum Evolution trees (Fig. 1). *Achroiostachys levigata* is most closely related to *Ac. humicola* in trees (Fig. 1), but the ITS-rDNA could well delineate the former from the latter species and all other accepted species in the genus *Achroiostachys*. The phylogeny shows that *Ac. humicola* forming a well-supported clade with 95/0.96 bootstrap close to *Ac. levigata* (Fig. 1).

The two species can be distinguished morphologically by conidium size ((-7) 7.5–8.5(-10) × (-5) 5.5–6.5(-7) μm (av. 8 × 6 μm)) in *Ac. humicola* vs. (-7) 8.5–9.5 (-10) × (-6) 6.5–7.5 (-8) μm (mean = 9 × 7 μm) in *Ac. levigata*, in which *Ac. levigata* produces broader conidia than *Ac. humicola*. In addition, *Ac. humicola* can also be morphologically distinguished from other species of the genus by having shorter conidiophores (up to 65 μm in *Ac. humicola* vs. up to 70 μm in *Ac. phyllophila*, up to 75 μm in *A. levigata*, up to 85 μm in *Ac. betulicola*, and up to 140 μm in *Ac. saccharicola*).

There are only a few reports of *Ac. humicola* worldwide (Lombard et al. 2016) that of from soil under *Zea mays* in Canada, from agricultural soil in the Netherlands, and a unknown substrate in Turkey. This is the first report of the isolation of this species as an endophyte from a plant species. So, this survey provided new insights into the distribution of this species.

***Cephalotrichum tenuissimum* Woudenb. & Seifert, Studies in Mycology 88: 149 (2017). Fig. 4.**

Culture characteristics. Colonies on PDA are olivaceous grey, becoming dark gray with age, with olivaceous grey synnemata, margins irregular, reaching 50 mm diam in 14 d at 25 °C. Sporulation initiates in the center and extends to the margins. Sporulation in PDA is much less than PCA and MEA.

Sexual morph absent. Conidiomata synnemata, mononematous conidiophores biverticillate to terverticillate but often irregular, commonly form among synnemata, bearing 3–5 annellides on cylindrical or swollen metulae 5.5–8.5 × 2–3 μm; branches divergent, 8–12 × 2–3 μm; stipe 5–20(-70) × 2–3 μm. Synnemata 500–900 μm in height, stipes pale brown to brown, 14–24 μm in width, conidial heads obclavate, pale brown. Setae absent. Hyphae of stipe brown, parallel, 1.5–2.5 μm in width. Conidiogenous cells are hyaline, smooth-walled, ampulliform, 5–8.5 × 2.5–3.5 μm, broad at the widest part, tapering gradually to a cylindrical annellated zone, sometimes forming in groups of 2–3 on short metulae. Conidia hyaline to pale green-brown, smooth, thick-walled, single or in short chains, ellipsoidal with truncate base and rounded apex, 4.5–6.5 × 3–4 μm.

Specimens examined. IRAN. West Azarbaijan: Urmia (37.44020, 45.12455), from the root of *Ph.*

australis, Oct-2018, Fatemeh Salimi & Alireza Alizadeh, culture FS-W4P4R3.

Note: The strain examined in this study shows similar morphology to that described by Woudenberg et al. (2017) for *C. tenuissimum*. In blastn searches of NCBI GenBank, the ITS sequence of isolate FS-W4P4R3 matched with 99.81% identity to an ex-type strain of *C. tenuissimum* (CBS 127792).

The strain examined confidently clustered with the type strain of *C. tenuissimum* (CBS 127792) in both Bayesian and Minimum evolution trees (Fig. 1). *C. dendrocephalum* and *C. hinnuleum* have the closest relationship with *C. tenuissimum* in the trees (Fig. 1), but the ITS-rDNA could well delineate this species from this species and all accepted taxa in the genus *Cephalotrichum*. The investigated isolate was confidently clustered with the type strain of *C. tenuissimum* (CBS 127792) in both Bayesian and Minimum Evolution trees (Fig. 1). *Cephalotrichum dendrocephalum* and *C. hinnuleum* are most closely related to *C. tenuissimum* in trees (Fig. 1), but the ITS-rDNA could well delineate this species from these two species and all other accepted species in the genus *Cephalotrichum*.

Cephalotrichum tenuissimum and *C. hinnuleum* are two closely related species in our phylogenetic analyses, which can also be distinguished morphologically by the formation of straight setae in *C. dendrocephalum* and the absence of setae in *C. tenuissimum*. *C. hinnuleum* is easily distinguished from *C. tenuissimum* by producing an echinobotryum-like syn-aseexual morph, larger (8–10 × 5.5–7 μm in *C. hinnuleum* vs. 4.5–6.5 × 3–4 μm in *C. tenuissimum*) and unbeaked, echinobotryum-like conidia and the presence of a non-diffusible brown pigment in the colony reverse on PDA.

Little is known about the biodiversity of *Cephalotrichum* species in Iran and there are a few reports of species of this genus, which include *C. microsporium* as endophyte from apple trees (Alijani et al. 2016), *C. oligotrophicum* from *Robinia pseudoacacia* (Paripour et al. 2019).

C. nanum from shoots of apple trees and leaf debris of apple and ash, *C. asperulum* from leaf debris of apple and sycamore and stem debris of reed plants (Ghosh et al. 2020), *C. asperulum* and *C. gorgonifer* from the decayed root of pistachio (Alizadeh et al. 2021) and *C. tenuissimum* as endophyte from potato (Alijani et al. 2022).

Cephalotrichum tenuissimum was first reported from Iran as an endophytic fungus from leaves, stems, roots and tubers of potatoes in the south of Kerman province (Alijani et al. 2022). However, little is known about its geographic distribution and host range. The present study introduces *Ph. australis* as a new host for *C. tenuissimum* and provides new insights into the host range and distribution of this species.

Myrmecridium schulzeri (Sacc.) Arzanlou, W. Braun, Shin & Crous, *Stud. Mycol.* 58: 84 (2007). Fig. 5.

Cultural characteristics. Colonies on PDA flat, rather compact with the entire margin, surface dark brown at the center and orange in the margin, becoming farinose or powdery with age due to sporulation, which causes concentric zones after a while, 29 mm diam in 7 d at 25 °C, reverse the same.

Hyphae hyaline, thin-walled, 1–2 µm wide, aerial hyphae pale olivaceous-brown. Conidiophores reddish brown, straight, unbranched, thick-walled, septate, up to 270 µm high, 2.5–3.5 µm tall, basal cell regularly inflated, 3.5–5 µm wide.

Conidiogenous cells are cylindrical, integrated, variable in length, 30–110 µm long, subhyaline to pale brown, fertile part subhyaline, forming a straight rachis with scattered, pimple-shaped denticles (< 1 µm long and < 0.5 µm wide), apically pointed, slightly thickened scars. Conidia solitary, subhyaline, obovoid, thin-walled, smooth or finely verrucose, 6–12 × 3–4 µm, tapering to a sub-truncate base; hilum pigmented, easily visible in the base.

Specimens examined. IRAN. East Azarbaijan: Sharafkhane (38.11361, 45.28190), from the root of *Phragmites australis*, Oct-2018, Fatemeh Salimi & Alireza Alizadeh, culture FS-N1P6S1; IRAN. East Azarbaijan: Sharafkhane (38.11361, 45.28190), from the root of *Ph. australis*, Oct-2018, Fatemeh Salimi & Alireza Alizadeh, culture FS-UN7.

Notes: The morphology of this fungus fully agrees with the description available in *Myrmecridium schulzeri* Arzanlou, W. Gams & Crous (Arzanlou et al. 2007). The isolate examined here FS-N1P6S1 and FS-UN7 confidently clustered in a well-supported clade with reference and type strain of *M. schulzeri* (CBS 325.74) in both Bayesian and Minimum Evolution trees (Fig. 1).

The morphology of this fungus fully matches the description of *M. schulzeri* Arzanlou, W. Gams & Crous (Arzanlou et al. 2007). The isolates examined here, FS-N1P6S1 and FS-UN7, were confidently grouped into a well-supported clade with reference strains and ex-type of *M. schulzeri* (CBS 325.74) in both Bayesian and Minimum Evolution trees (Fig. 1).

Little is known about the biodiversity of the genus *Myrmecridium* and its species in Iran and there is only one report of *M. schulzeri* in Iran that of from merged rotten leaves at Anzali lagoon (Rezakhani et al. 2019). The current study introduces *Ph. australis* as a new host for *M. schulzeri* and provides further insight into the host range and distribution of this species.

Periconia igniaria E.W. Mason & M.B. Ellis, *Mycological Papers* 56: 104 (1953). Fig. 6.

Culture characteristics. Colonies on PDA effuse with entire margin, surface white produce rose-madder or vinaceous pigments on media, reaching 45

mm diam in 7 d at 25 °C, reverse on PDA rose-madder or vinaceous.

Conidiophores macronematous, mononematous, determinate, smooth-walled, 4–8-septate, up to 450 µm tall, 7–9 µm wide immediately below the head, 9–13 µm wide at the base, 6–10 µm wide in the stipe, bearing shorter branches or stipes immediately below the head. Stipes erect, stout, smooth-walled, branched, pale brown, with bead-like appearance. Conidiogenous cells are holoblastic, spherical or subspherical, pale to mid-brown, smooth-walled, arising normally directly from the stipe, bearing simple or branched chains of conidia forming apically and laterally on the stipes, which form loose heads. Conidia aseptate, thick-walled, verruculose to echinulate, spherical, brown to dark brown, developing in acropetal chains, 7–10.5 µm diam.

Specimens examined. IRAN. East Azarbaijan: Sharafkhane (38.11361, 45.28190), from the leaf of *Phragmites australis*, July-2018, Fatemeh Salimi & Alireza Alizadeh, culture FS-N4P10L3; IRAN. East Azarbaijan: Sharafkhane (38.11361, 45.28190), from the leaf of *Ph. australis*, July-2018, Fatemeh Salimi & Alireza Alizadeh, culture FS-N3P7L4; IRAN. East Azarbaijan: Sharafkhane (38.11361, 45.28190), from the stem of *Ph. australis*, July-2018, Fatemeh Salimi & Alireza Alizadeh, culture FS-N3P3S2; IRAN. East Azarbaijan: Sharafkhane (38.11361, 45.28190), from the leaf of *Ph. australis*, July-2018, Fatemeh Salimi & Alireza Alizadeh, culture FS-N6P4L2; IRAN. East Azarbaijan: Sharafkhane (38.11361, 45.28190), from the root of *Ph. australis*, July-2018, Fatemeh Salimi & Alireza Alizadeh, culture FS-N3P4R8; IRAN. East Azarbaijan: Sharafkhane (38.11361, 45.28190), from the leaf of *Ph. australis*, July-2018, Fatemeh Salimi & Alireza Alizadeh, culture FS-N3P2L3; IRAN. East Azarbaijan: Sharafkhane (38.11361, 45.28190), from the stem of *Ph. australis*, July-2018, Fatemeh Salimi & Alireza Alizadeh, culture FS-N3P8S1; IRAN. East Azarbaijan: Sharafkhane (38.11361, 45.28190), from the root of *Ph. australis*, July-2018, Fatemeh Salimi & Alireza Alizadeh, culture FS-N3P2R1; IRAN. East Azarbaijan: Sharafkhane (38.11361, 45.28190), from the leaf of *Ph. australis*, July-2018, Fatemeh Salimi & Alireza Alizadeh, culture FS-N4P10L3.

Notes: The morphology of this fungus fully agrees with the description available in *P. igniaria*, Ellis (1971). The isolates examined here (FS-N3P4R10, FS-N3P7L4, FS-N3P3S2, FS-N6P4L2, FS-N3P4R8, FS-N3P2L3, FS-N3P8S1, FS-N3P2R1 and FS-N4P10L3) confidently clustered in a well-supported clade with valid reference strains and type strains of *P. igniaria* (CBS 379.86) in both Bayesian and Minimum Evolution trees (Fig. 1). Phylogenetic analyses based on ITS-rDNA could well delineate this species from all accepted taxa in the genus *Periconia*.

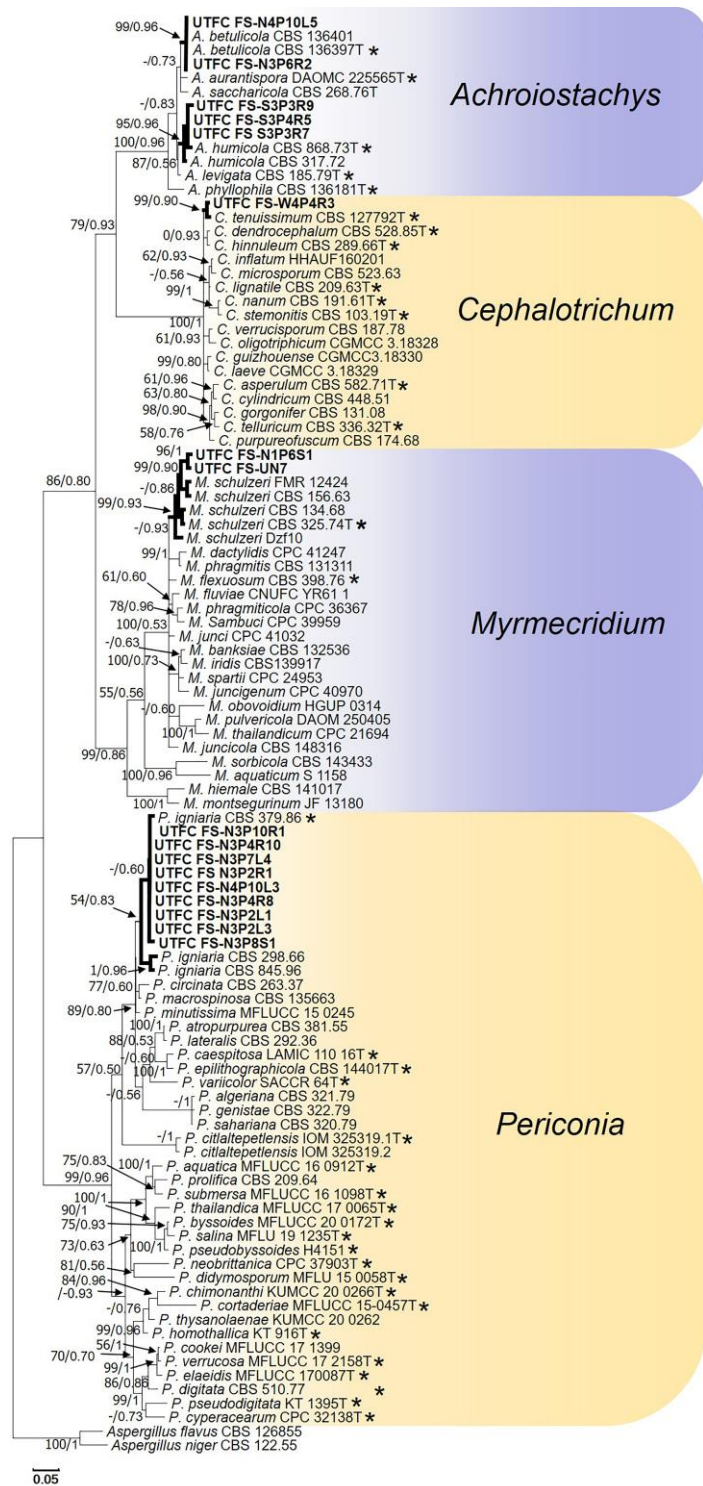


Fig. 1. Phylogram generated from Bayesian analysis based on ITS sequence data. Bootstrap support values above 50 % and Bayesian posterior probability values above 0.70 are shown at the nodes as ME/PP. *Aspergillus flavus* strain CBS 126855 and *A. niger* strain CBS 122.55 are used as outgroups. The newly generated strains in this study are in bold and ex-type strains are emphasized with an asterisk (*).

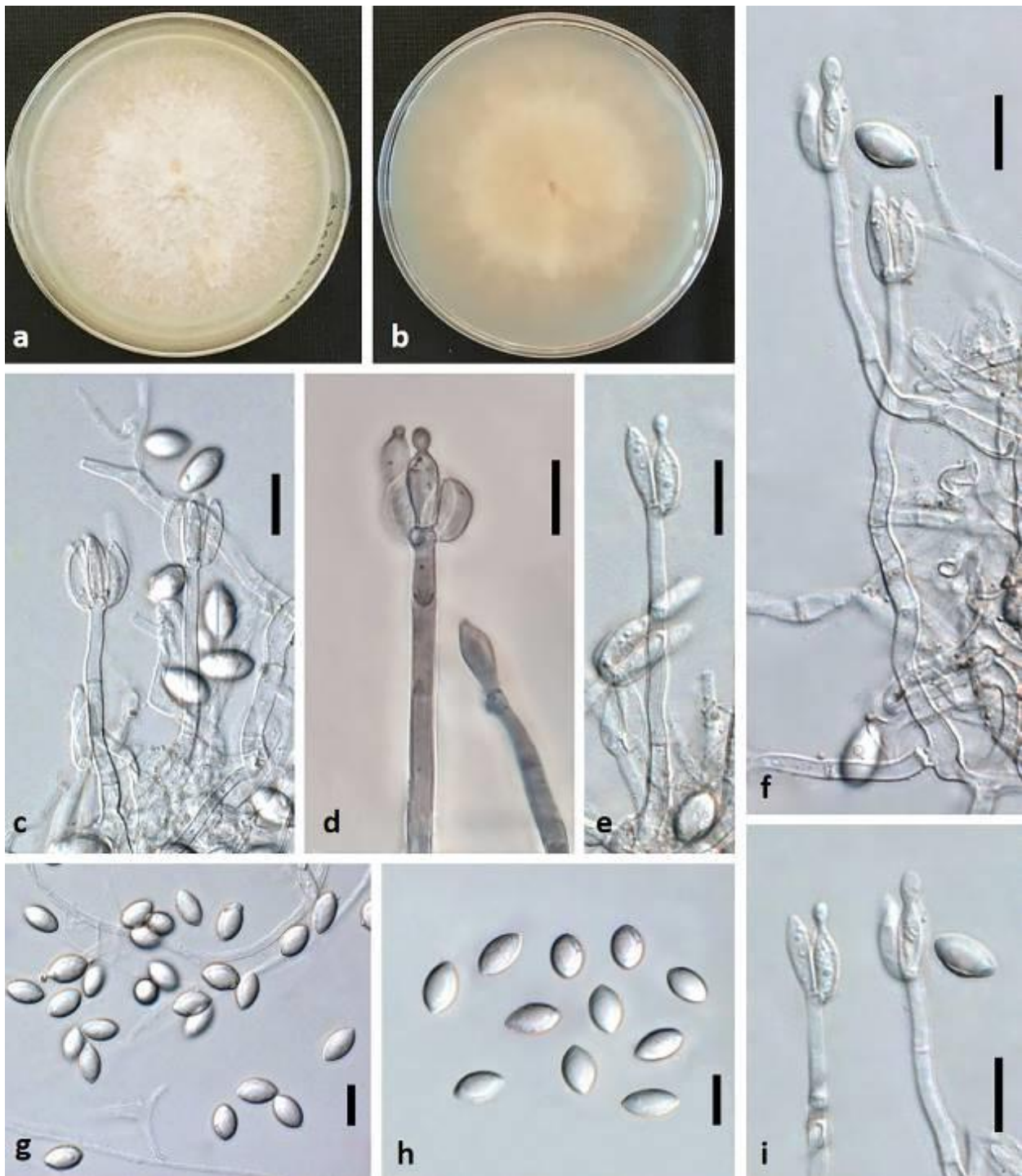


Fig. 2. *Achroiostachys betulicola* (isolate FS-N4P10L5). **a–b.** Colony on PDA after 7 d, **a.** upper and **b.** reverse side. **c–f, i.** Conidiophores; **g–h.** conidia. Scale bars = 10 μ m.

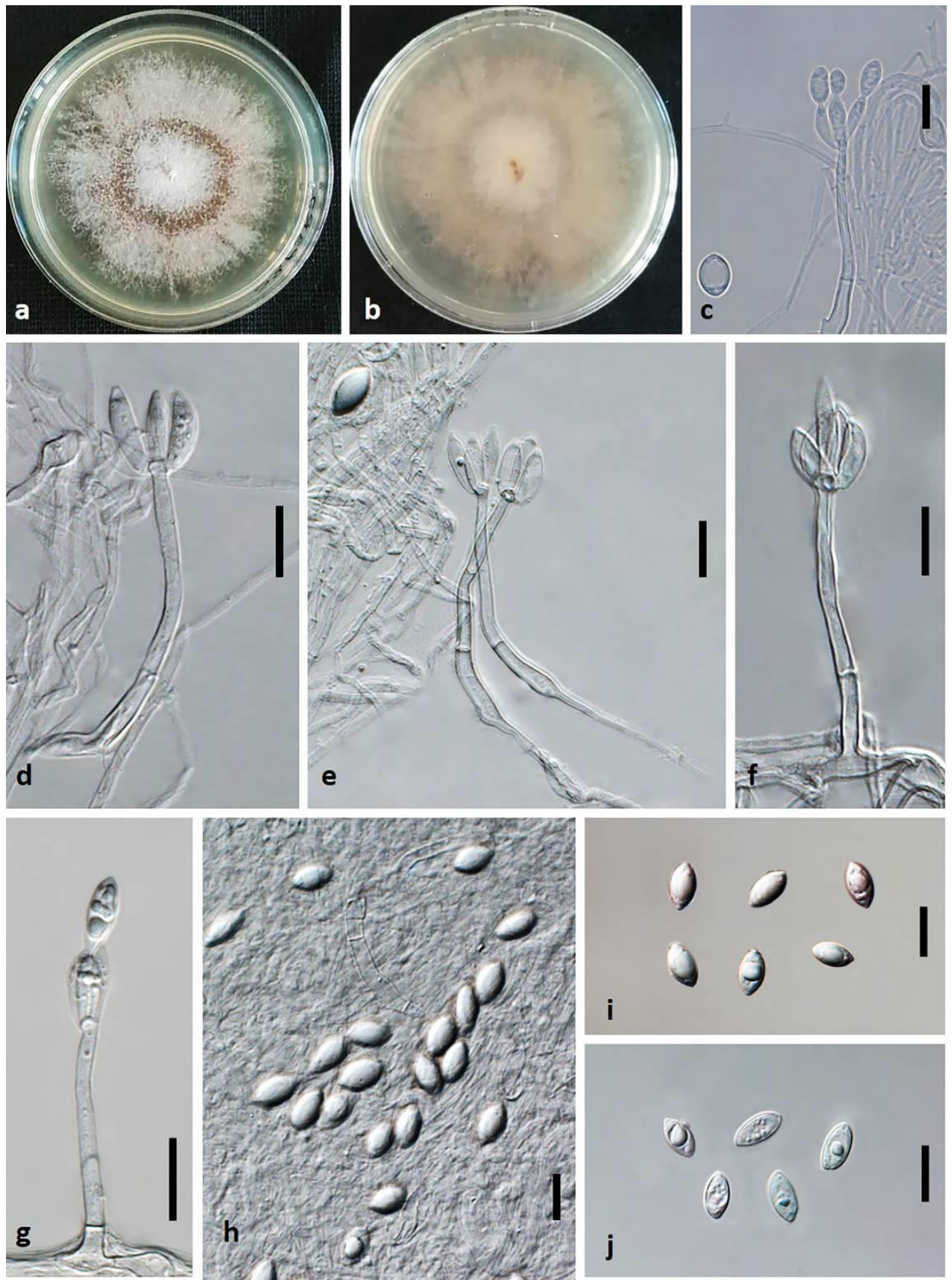


Fig. 3. *Achroiostachys humicola* (isolate FS-S3P3R9). **a–b.** Colony on PDA after 7 d, **a.** Upper and **b.** Reverse side. **c–g.** Conidiophores; **h–j.** Conidia. Scale bars = 10 μ m.

This species is abundantly isolated from soil and air and from a wide range of plants including *Phragmites australis*, *Quercus ilex*, *Rosmarinus officinalis*, *Scirpus maritimus*, *Vitis* sp., *Vitis vinifera* in Spain, *Centaurea solstitialis* and *Phalaroides arundinacea* in Russia, *Diplotaxis eruroides* in Spain, from *Juncus*

roemerianus in Florida, *Medicago sativa* in South Africa (Farr & Rossman 2021). Asgari & Zare (2004) reported this species from barley leaves for the first time in Iran using morphological characteristics. This study is the first report of *P. igniaria* in Iran with molecular confirmation through DNA sequencing

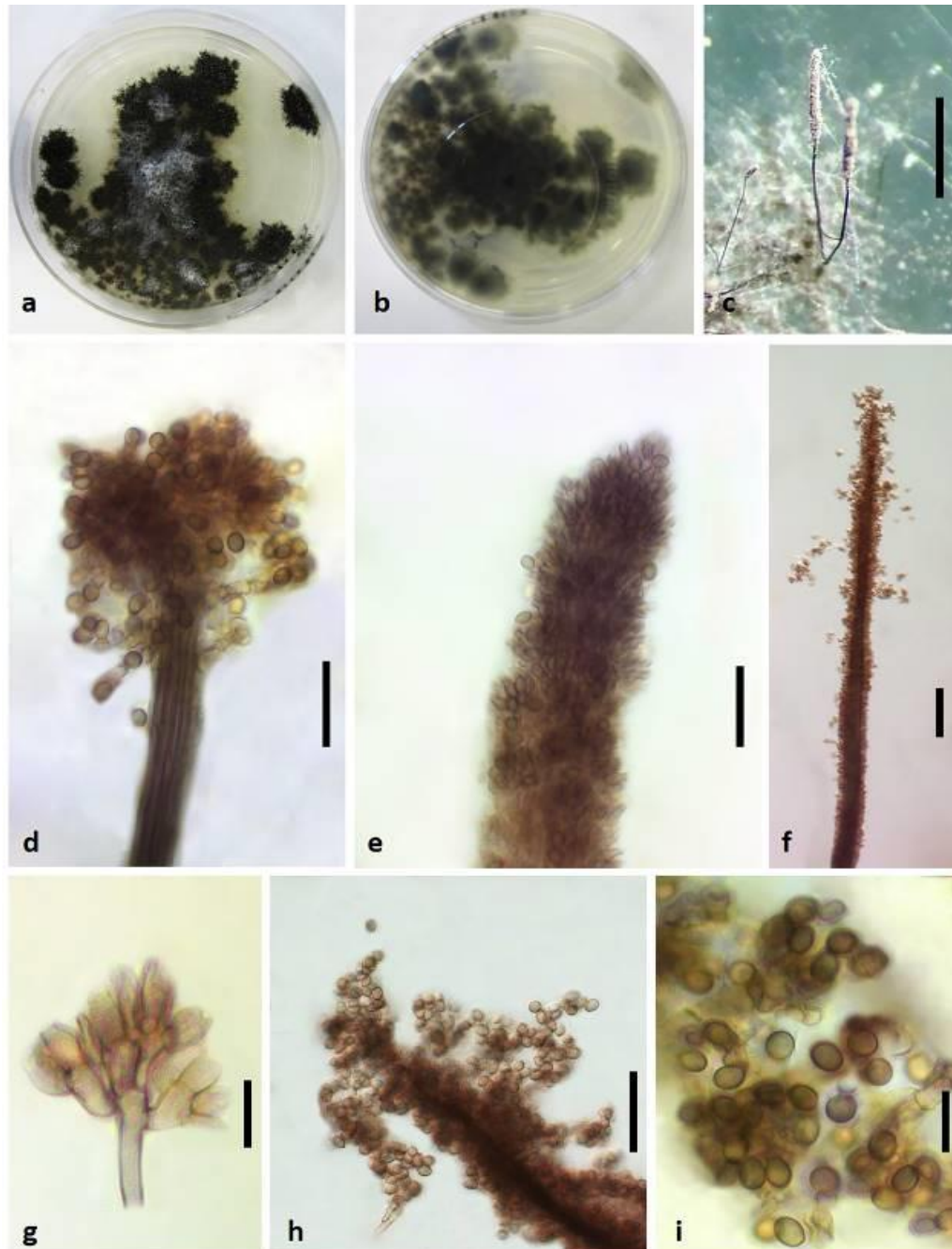


Fig. 4. *Cephalotrichum tenuissimum* (isolate FS-W4P4R3). **a–b.** Colony on PDA after 7 d, **a.** Upper and **b.** Reverse side. **c.** Synnema. **d–f.** The apical portion of a synnema. **g.** Detail of the apical portion of a synnema and conidiogenous cells. **h–i.** Conidia. Scale bars: **c** = 500 μm , **d–f, h** = 50 μm , **g, i** = 10 μm .

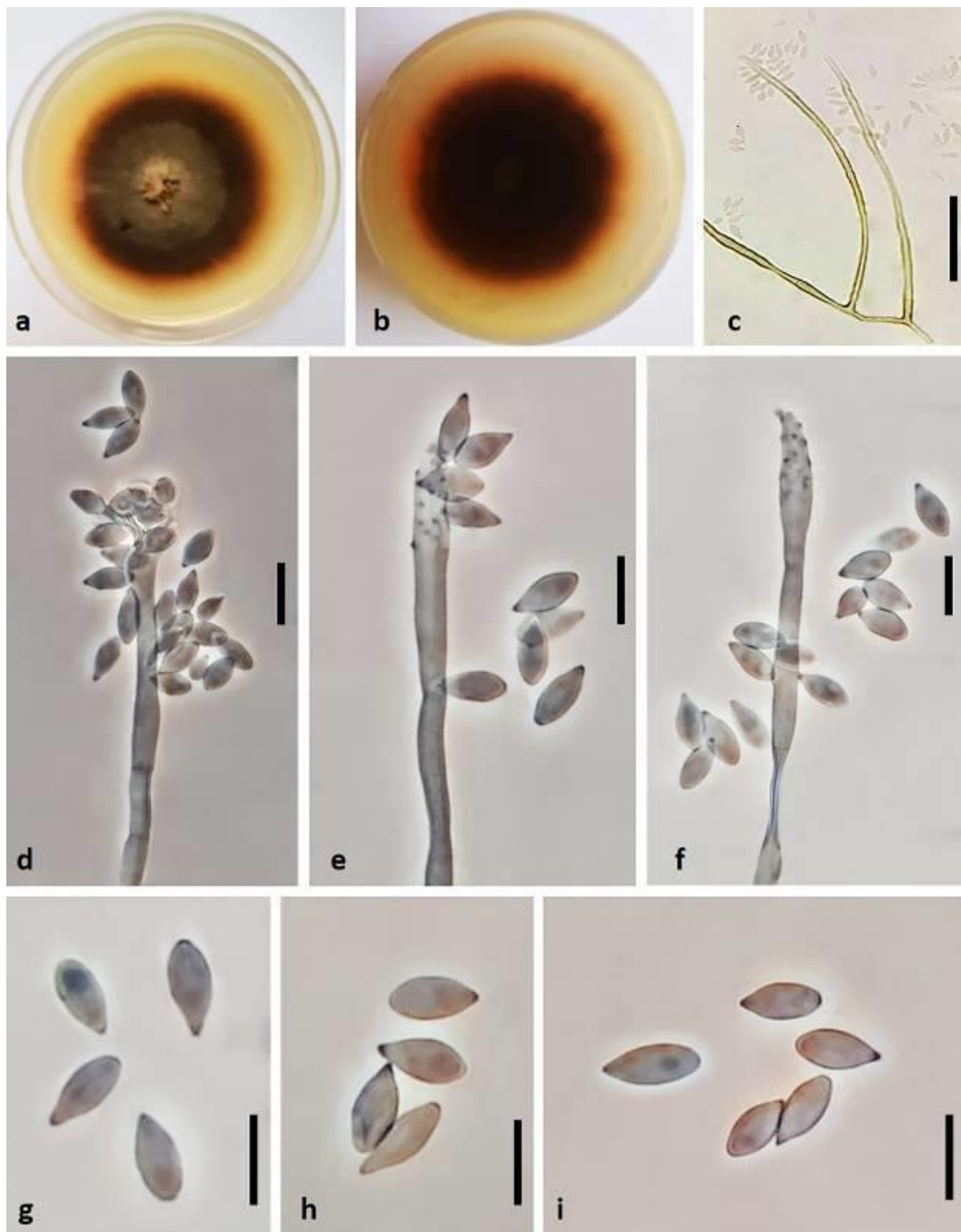


Fig. 5. *Myrmecridium schulzeri* (isolate FS-N1P6S1). **a–b.** Colony on PDA after 7 d, **a.** Upper and **b.** Reverse side. **c.** Macronematous conidiophores. **d–e.** The apical portion of conidiophore, conidial development in macronematous conidiophores and sympodially proliferating conidiogenous cells. **f.** Rachis with scattered, pimple-shaped denticles. **g–i.** Conidia. Scale bars: **c** = 50 μ m, **d–i** = 10 μ m.

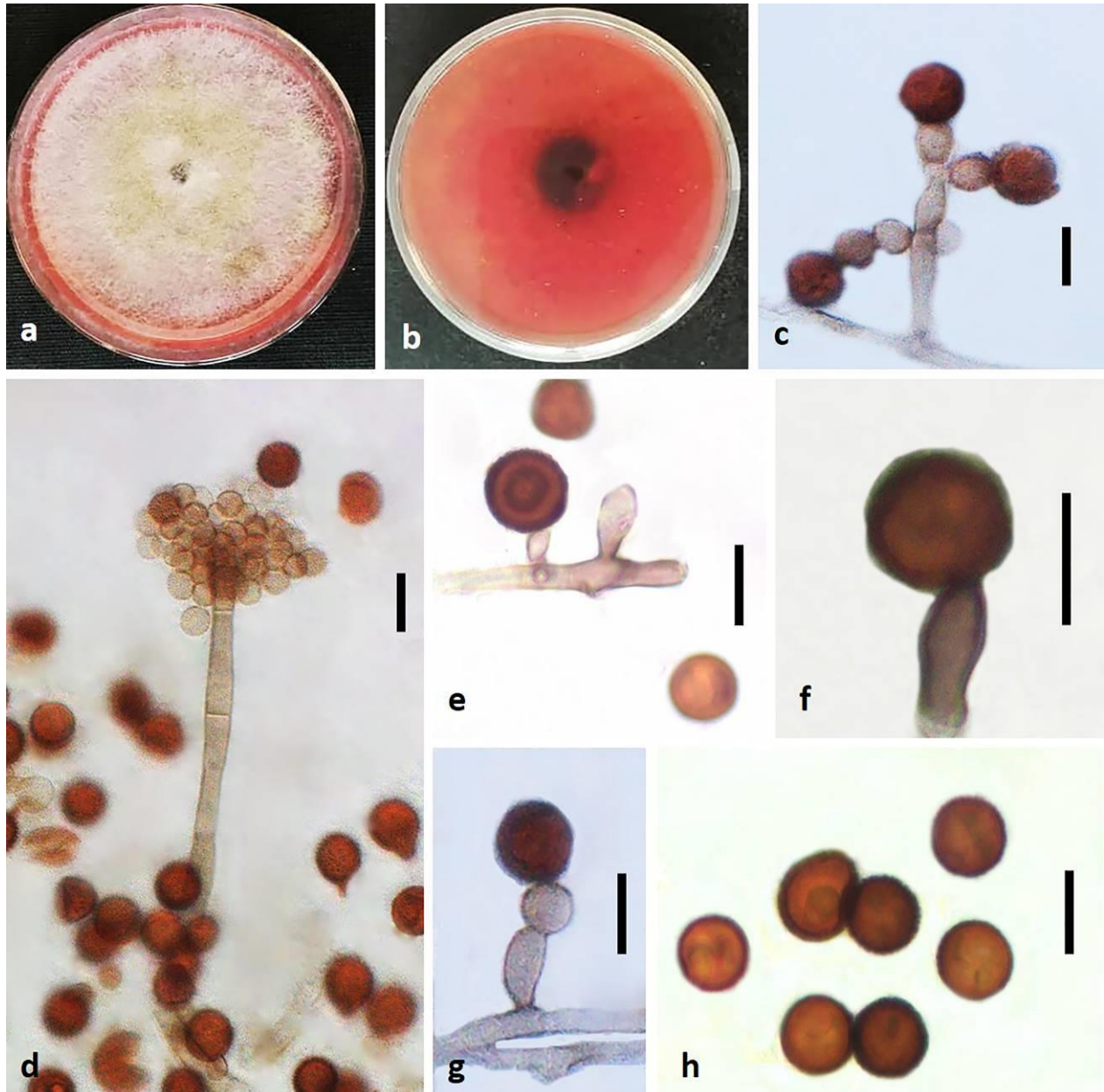


Fig. 6. *Periconia igniaria* (isolate FS-N4P10L3). **a–b.** Colony on PDA after 7 d, **a.** Upper and **b.** Reverse side. **c.** A Branched conidiophore with a bead-like appearance. **d.** Conidiophore aggregates with conidia. **e–g.** Conidiogenous cell bearing conidia. **h.** Conidia. Scale bars = 10 µm.

DISCUSSION

Investigation of seventeen endophytic fungal isolates recovered from leaves, stems and healthy roots of *Ph. australis* collected from five different sites around Lake Urmia in Iran, showed that the isolates belong to five morphotypes, based on colony characteristics and micromorphology. Detailed morphological examination and phylogeny inferred from nuclear ribosomal internal transcribed spacer sequence (ITS-rDNA) showed that the isolates belong to five different species namely *Achroistachys betulicola*, *Ac. humicola*, *Cephalotrichum tenuissimum*, *Myrmecridium schulzeri*, and *Priconia igniaria*. Based on ITS-rDNA sequence data the identified

species could be differentiated from all confirmed species of the respective genera. To the best of our knowledge, this is the first report of *Ac. betulicola* and *Ac. humicola* for Funga of Iran. Also, the presence of *P. igniaria* in Iran was confirmed for the first time with molecular characterization through DNA sequencing. With the second report of *C. tenuissimum*, *M. schulzeri* and *P. igniaria* in Iran, this study provided further new insights into the distribution and host range of the identified species. Today, the discovery of beneficial properties and positive aspects of endophytic fungi is increasing faster than ever (Busby et al. 2016; Card et al. 2016; Vega 2018; Quesada-Moraga 2020). Especially in recent years, due to climate change and its negative

consequences, which have caused heavy economic losses already, more attention has been directed toward the development of efficient and environmentally friendly methods to reduce the direct and indirect consequences of climate change and anthropogenic habitat alterations. This includes the potential of using fungal endophytes, to increase the tolerance of plants against a wide range of biotic and abiotic stresses (Rodriguez et al., 2008). While the full potential has been barely touched upon, already several effective biological products, including biofertilizers and pesticides, have been successfully applied to enhance plant growth and biological control of several pests and pathogens (Bamisile et al. 2019).

Although the history of research on plant endophytic fungal communities is long, the identification of endophytic fungi of more plant species, in divergent geographic regions and bioclimatic conditions is still in its infancy. So far, several fungal species have been isolated and reported from reed plants in Iran, which are listed in a comprehensive list of fungi along with their hosts in the book "Fungi of Iran" (Ershad 2021). However, none of the species identified here have been isolated and reported from reed plants in Iran before. This suggests that the host-microbe interaction of endophytic fungi with their plants can be significantly different from the situation on other hosts where disease symptoms develop. *Phragmites australis* is known as one of the most common and successful species in occupying lands around the world, and it has been suggested that its adaptation to a wide range of environmental conditions is can be related to the symbiotic relationship with endophytic microorganisms (Rodriguez et al. 2008, Kowalski et al. 2015; Sangamesh et al. 2018). Therefore, if the endophyte strains obtained from *P. australis* found in this study confer a greater tolerance to biotic or abiotic stresses, they might have the potential to be used to promote the yield of crops, such as barley, wheat, and maize in stressful habitats.

ACKNOWLEDGMENT

This study is supported by the Deputy of Research and Technology of the University of Tehran. Also, we gratefully acknowledge the Iran National Science Foundation (INSF) for financially supporting under grant number 97012471. The authors highly appreciate the great assistance of Sebastian Ploch, Laboratory Manager at Biodiversity and Climate Research Centre, Frankfurt, Germany in setting up the experiments and helpful comments.

REFERENCES

Aboul-Maaty NAF, Oraby HAS. 2019. Extraction of high-quality genomic DNA from different plant orders applying a modified CTAB-based method. *Bulletin of the National Research Centre* 43:1-10.

Achenbach L, Brix H. 2014. Can differences in salinity tolerance explain the distribution of four genetically distinct lineages of *Phragmites australis*

in the Mississippi River Delta? *Hydrobiologia* 737: 5-23.

Arzanlou M, Groenewald JZ, Gams W, Braun U, Shin HD, Crous PW. 2007. Phylogenetic and morphotaxonomic revision of *Ramichloridium* and allied genera. *Studies in Mycology* 58: 57-93.

Asgari B, Zare R, Payghami E. 2004. Hyphomycetous fungal community of barley phylloplane in East Azarbaijan province with emphasis on new taxa for Iranian fungal flora. *Rostaniha* 52: 171-198.

Atala C, Acuña-Rodríguez IS, Torres-Díaz C, Molina-Montenegro MA. 2022. Fungal endophytes improve the performance of host plants but do not eliminate the growth/defense trade-off. *New Phytologist* 235: 384-387.

Bamisile BS, Dash CK, Akutse KS, Keppanan R, Wang L. 2018. Fungal endophytes: beyond herbivore management. *Frontiers in Microbiology* 9: 544.

Baron NC, Rigobelo EC. 2022. Endophytic fungi: a tool for plant growth promotion and sustainable agriculture. *Mycology* 13: 39-55.

Bashyal BP, Burns AM, Liu MX, Paranagama PA, Seliga CJ, Turbyville TJ, Gunatilaka AAL. 2006. Discovery of small molecule bioactive agents from endophytic fungi of the Sonoran Desert NZGA. *Research and Practice Series* 13: 211-214.

Bills GF, González-Menéndez V, Martín J, Platas G, Fournier J, Peršoh D, Stadler M. 2012. Hypoxylon pulvicidum sp. nov. Ascomycota Xylariales a pantropical insecticide-producing endophyte. *PLoS ONE* 7: e46687.

Bonanno G, Giudice RL. 2010. Heavy metal bioaccumulation by the organs of *Phragmites australis* common reed and their potential use as contamination indicators. *Ecological Indicators* 10: 639-645.

Breen JP. 1994. Acremonium endophyte interactions with enhanced plant resistance to insects. *Annual Review of Entomology* 39: 401-423.

Brem D, Leuchtman A. 2001. Epichloë grass endophytes increase herbivore resistance in the woodland grass *Brachypodium sylvaticum*. *Oecologia* 126: 522-530.

Busby PE, Ridout M, Newcombe G. 2016. Fungal endophytes: modifiers of plant disease *Plant. Molecular Biology* 90: 645-655.

Card S, Johnson L, Teasdale S, Caradus J. 2016. Deciphering endophyte behaviour: the link between endophyte biology and efficacious biological control agents FEMS. *Microbiology Ecology* 92: 1-19.

Cheplick GP, Faeth S, Faeth SH. 2009. Ecology and evolution of the grass-endophyte symbiosis. Oxford University Press, USA.

Clay K, Schardl C. 2002. Evolutionary origins and ecological consequences of endophyte symbiosis with grasses. *The American Naturalist* 160: 99-127.

- Farr DF, Rossman AY. 2021. Fungal databases US National fungus collections ARS USDA [Retrieved August 3, 2021] Available online at <https://ntars-gringov/fungal/databases/>.
- Fér T, Hroudova Z. 2009. Genetic diversity and dispersal of *Phragmites australis* in a small river system *Aquatic Botany* 90: 165-171.
- Fisher PJ, Graf F, Petrini LE, Sutton BC, Wooley PA. 1995. Fungal endophytes of *Dryas octopetala* from a high arctic polar semidesert and from the Swiss Alps. *Mycologia* 87: 319-323.
- Harrington AH, del Olmo-Ruiz M, U'Ren JM, Garcia K, Pignatta D, Wespe N, Arnold AE. 2019. *Coniochaeta endophytica* sp. nov. a foliar endophyte associated with healthy photosynthetic tissue of *Platycladus orientalis* Cupressaceae. *Plant and Fungal Systematics* 64: 65-79.
- Hyde KD, Soyong K. 2008. The fungal endophyte dilemma. *Fungal Diversity* 33: 163-173.
- Ibrahim A, Tanney JB, Fei F, Seifert KA, Cutler GC, Capretta A, Sumarah MW. 2020. Metabolomic-guided discovery of cyclic nonribosomal peptides from *Xylaria ellisii* sp. nov. a leaf and stem endophyte of *Vaccinium angustifolium*. *Scientific Reports* 10: 1-17.
- Katoh K, Standley DM. 2013. MAFFT multiple sequence alignment software version 7: improvements in performance and usability. *Molecular Biology and Evolution* 30: 772-780.
- Katoh K, Rozewicki J, Yamada KD. 2019. MAFFT online service: multiple sequence alignment interactive sequence choice and visualization. *Briefings in Bioinformatics* 20: 1160-1166.
- Kipfer T, Moser B, Egli S, Wohlgenuth T, Ghazoul J. 2011. Ectomycorrhiza succession patterns in *Pinus sylvestris* forests after stand-replacing fire in the Central Alps. *Oecologia* 167: 219-228.
- Kowalski KP, Bacon C, Bickford W, Braun H, Clay K, Leduc-Lapierre M, Wilcox DA. 2015. Advancing the science of microbial symbiosis to support invasive species management: a case study on *Phragmites* in the Great Lakes. *Frontiers in Microbiology* 6: 1-14.
- Li HY, Shen M, Zhou ZP, Li T, Wei YL, Lin LB. 2012. Diversity and cold adaptation of endophytic fungi from five dominant plant species collected from the Baima Snow Mountain Southwest China. *Fungal Diversity* 54: 79-86.
- Liu AR, Xu T, Guo LD. 2007. Molecular and morphological description of *Pestalotiopsis hainanensis* sp. nov. a new endophyte from a tropical region of China. *Fungal Diversity* 24: 23-36.
- Lombard L, Houbaken J, Decock C, Samson RA, Meijer M, Réblová M, Crous PW. 2016. Generic hyper-diversity in *Stachybotriaceae*. *Persoonia-Molecular Phylogeny and Evolution of Fungi* 36: 156-246.
- Mason EW, Ellis MB. 1953. British species of *Periconia*. *Mycological Papers* 56: 104.
- Meshram V, Kapoor N, Saxena S. 2013. *Muscodor kashayum* sp. nov.—a new volatile anti-microbial producing endophytic fungus. *Mycology* 44: 196-204.
- Meyerson LA, Cronin JT, Pyšek P. 2016. *Phragmites australis* as a model organism for studying plant invasions *Biological Invasions* 18: 2421-2431.
- Noumeur SR, Teponno RB, Helaly SE, Wang XW, Harzallah D, Houbaken J, Stadler M. 2020. Diketopiperazines from *Batnamyces globulariicola* gen. & sp. nov. *Chaetomiaceae* a fungus associated with roots of the medicinal plant *Globularia alypum* in Algeria. *Mycological Progress* 19: 589-603.
- Novas MV, Carmarán CC. 2008. Studies on diversity of foliar fungal endophytes of naturalised trees from Argentina with a description of *Haplotrichum minutissimum* sp. nov. *Flora-Morphology Distribution Functional Ecology of Plants* 203: 610-616.
- Preethi K, Manon Mani V, Lavanya N. 2021. Endophytic fungi: A potential source of bioactive compounds for commercial and therapeutic applications. In: *Endophytes: Potential Source of Compounds of Commercial and Therapeutic Applications*. (Patil RH, Maheshwari VL): 247-272. Springer Press, Singapore.
- Price MN, Dehal PS, Arkin AP. 2010. FastTree 2—approximately maximum-likelihood trees for large alignments. *PLoS One* 53: e9490.
- Quesada Moraga E. 2020. Entomopathogenic fungi as endophytes: their broader contribution to IPM and crop production *Biocontrol Science and Technology* 30: 864-877.
- Redman RS, Sheehan KB, Stout RG, Rodriguez RJ, Henson JM. 2002. Thermotolerance generated by plant/fungal symbiosis. *Science* 298: 1581-1581.
- Rezakhani F, Khodaparast SA, Masigol H, Roja-Jimenez K, Grossart HP, Bakhshi M. 2019. A preliminary report of aquatic hyphomycetes isolated from Anzali lagoon Gilan province North of Iran. *Rostaniha* 202: 123-143.
- Rodriguez RJ, Henson J, Van Volkenburgh E, Hoy M, Wright L, Beckwith F, Redman RS. 2008. Stress tolerance in plants via habitat-adapted symbiosis. *The ISME Journal* 2: 404-416.
- Ronquist F, Teslenko M, Van Der Mark P, Ayres DL, Darling A, Höhna S, Huelsenbeck JP. 2012. MrBayes 3.2: efficient Bayesian phylogenetic inference and model choice across a large model space. *Systematic Biology* 61: 539-542.
- Rosa LH, Vaz A, Caligiorno RB, Campolina S, Rosa CA. 2009. Endophytic fungi associated with the Antarctic grass *Deschampsia antarctica* DesvPoaceae. *Polar Biology* 32: 161-167.
- Salimi F, Alizadeh A, Mirzadi Gohari A, Javan-Nikkhah M. 2019. Endophytic fungus *Radulidium subulatum* from *Phragmites australis* in Iran. *Mycologia Iranica* 6: 41-47.
- Sangamesh MB, Jambagi S, Vasanthakumari MM, Shetty NJ, Kolte H, Ravikanth G, Uma Shaanker

- R. 2018. Thermotolerance of fungal endophytes isolated from plants adapted to the Thar Desert India. *Symbiosis* 75: 135-147.
- Schulz B, Boyle C, Draeger S, Römmert AK, Krohn K. 2002. Endophytic fungi: a source of novel biologically active secondary metabolites. *Mycological Research* 106: 996-1004.
- Silva RM, Oliveira RJ, Bezerra JD, Bezerra JL, Souza-Motta CM, Silva GA. 2019. *Bifusisporella sorghi* gen. et sp. nov. Magnaporthaceae to accommodate an endophytic fungus from Brazil. *Mycological Progress* 18: 847-854.
- Singh A, Singh DK, Kharwar RN, White JF, Gond SK. 2021. Fungal endophytes as efficient sources of plant-derived bioactive compounds and their prospective applications in natural product drug discovery: Insights avenues and challenges. *Microorganisms* 9: 197.
- Soares MA, Li HY, Kowalski KP, Bergen M, Torres MS, White JF. 2016. Evaluation of the functional roles of fungal endophytes of *Phragmites australis* from high saline and low saline habitats. *Biological Invasions* 18: 2689-2702.
- Stamatakis A. 2014. RAxML version 8: a tool for phylogenetic analysis and post-analysis of large phylogenies. *Bioinformatics* 30: 1312-1313.
- Strobel GA. 2002. Rainforest endophytes and bioactive products *Critical Reviews in Biotechnology* 22: 315-333.
- Suryanarayanan TS, Wittlinger SK, Faeth SH. 2005. Endophytic fungi associated with cacti in Arizona. *Mycological Research* 109: 635-639.
- Tanney JB, Seifert KA. 2019. *Trybliopsis magnesii* sp. nov. from *Picea glauca* in Eastern Canada. *Fungal Systematics and Evolution* 4: 13-20.
- Tao G, Liu ZY, Liu F, Gao YH, Cai L. 2013. Endophytic *Colletotrichum* species from *Bletilla ochracea* Orchidaceae with descriptions of seven new species. *Fungal Diversity* 61: 139-164.
- Tutte J. 1969. *Plant pathological methods: Fungi and Bacteria*. Burgess Publishing, USA.
- Vega FE. 2018. The use of fungal entomopathogens as endophytes in biological control: a review. *Mycologia* 110: 4-30.
- Verma VC, Gangwar M, Yashpal M, Nath G. 2013. Anticestodal activity of endophytic *Pestalotiopsis* sp. on protoscoleces of hydatid cyst *Echinococcus granulosus*. *BioMed Research International* 2013: 308515.
- Wang JW, Wu JH, Huang WY, Tan RX. 2006. Laccase production by *Monotropa* sp. an endophytic fungus in *Cynodon dactylon*. *Bioresource Technology* 97: 786-789.
- White TJ, Bruns T, Lee S, Taylor J. 1990. Amplification and direct sequencing of fungal ribosomal RNA genes for phylogenetics. In: *PCR protocols: a guide to methods and applications*. (Innis MA, Gelfand DH, Sninsky JJ, and White TJ.): 315-322. Academic Press, USA.
- Woudenberg JHC, Sandoval-Denis M, Houbraken J, Seifert KA, Samson RA. 2017. *Cephalotrichum* and related synnematosus fungi with notes on species from the built environment. *Studies in Mycology* 87: 257-421.
- Yadav G, Meena M. 2021. Bioprospecting of endophytes in medicinal plants of Thar Desert: An attractive resource for biopharmaceuticals. *Biotechnology Reports* 30: e00629.
- Yang EF, Phookamsak R, Jiang HB, Tibpromma S, Bhat DJ, Karunaratna SC, Promputtha I. 2022. Taxonomic reappraisal of Periconiaceae with the description of three new Periconia species from China. *Journal of Fungi* 8: 243.
- Zhang CL, Liu SP, Lin FC, Kubicek CP, Druzhinina IS. 2007. *Trichoderma taxi* sp. nov. an endophytic fungus from Chinese yew *Taxus mairei*. *FEMS Microbiology Letters* 270: 90-96.
- Zheng H, Yu Z, Jiang X, Fang L, Qiao M. 2022. Endophytic *Colletotrichum* species from aquatic plants in southwest China. *Journal of Fungi* 81: 87-115.

گزارش جدیدی از قارچ‌های اندوفیت از گیاه نی (*Phragmites australis*) در ایران

فاطمه سلیمی^۱، محمد جوان نیکخواه^۱✉، علیرضا علیزاده^۲، امیر میرزادی گوهری^۱، مارکو تینس^۳

۱- گروه گیاهپزشکی، دانشکده کشاورزی، دانشگاه تهران، کرج، ایران.

۲- گروه گیاهپزشکی، دانشکده کشاورزی، دانشگاه شهید مدنی آذربایجان، تبریز، ایران.

۳- مرکز تحقیقات تنوع زیستی و اقلیم موسسه زنکنبرگ، فرانکفورت، آلمان و دانشگاه گوته، موسسه اکولوژی، تکامل و تنوع، فرانکفورت، آلمان

چکیده: به منظور شناسایی قارچ‌های اندوفیت گیاه نی (*Phragmites australis* (Poaceae) هفده جدایه از نمونه‌های برگ، ساقه و ریشه گیاهان نی سالم و بدون علائم، جمع‌آوری شده از پنج مکان مختلف در اطراف دریاچه ارومیه در استان‌های آذربایجان شرقی و غربی، جداسازی شد. پنج گونه مختلف به نام‌های *Cephalotrichum Ac. humicola*، *Achroistachys betulicola*، *Periconia igniaria* و *Myrmecridium schulzeri tenuissimum* بر اساس صفات ریخت‌شناختی و تجزیه و تحلیل تبارزایی توالی ناحیه ژنومی ITS-rDNA شناسایی شدند. بر اساس اطلاعات موجود، این اولین گزارش از گونه‌های *Ac. betulicola* و *Ac. humicola* برای فهرست قارچ‌های ایران می‌باشد. همچنین، این مطالعه اطلاعات جدیدی در مورد پراکنش جغرافیایی و دامنه میزبانی گونه‌های شناسایی شده را ارائه می‌نماید.

کلمات کلیدی: آسکومیکوتا، تنوع زیستی، تیره گندمیان، دریاچه ارومیه، فیلوژنی، همزیستی.